

Quality assessment of high performance concrete using digitized image elements

Sheng-Szu Peng¹, Edward H. Wang^{*1}, Her-Yung Wang² and Yu-Te Chou²

¹Minghsin University of Science and Technology, Hsin-Chu, Taiwan

²National Kaohsiung University of Applied Sciences, Kaohsiung, Taiwan

(Received April 17, 2011, Revised January 20, 2012, Accepted April 24, 2012)

Abstract. The quality of high performance concrete largely depends on water cement ratio, porosity, material composition and mix methods. The uniformity of color, texture and compressive strengths are quality indicators commonly used to assess the overall characteristics of concrete mixes. The homogeneity and share of coarse aggregates play a key role in concrete quality and must be analyzed in a microscopic point of view. This research studies the quality of high performance concrete by taking drilled cores in both horizontal and vertical directions from a 1.0 m³ specimen. The coarse aggregate, expressed in digitized 100×116 dpi resolution images are processed based on brightness in colors through commercial software converted into text files. With the image converting to text format, the share of coarse aggregate is quantified leading to a satisfactory assessment of homogeneity – a quality index of high performance concrete. The compressive strengths of concrete and the shares of coarse aggregate of the samples are also compared in this research study to illustrate its correlation in concrete quality. It is concluded that a higher homogeneity of aggregate exists in the vertical plane than that of the horizontal planes of the high performance concrete. In addition, the concrete specimen showing denser particle packing has relatively higher compressive strengths. The research methodology provides an easy-to-use, direct measurement of high performance concrete when conducting quality assessment in the construction site.

Keywords: image elements; high performance concrete; homogeneity; ANOVA.

1. Introduction

Aggregates account for 60-75% of the total volume in high performance concrete. Factors such as material properties, aggregate shapes, texture and maximum aggregate sizes, as well as aggregate particle packing have a significant impact on concrete strengths (Wang 1999). The time-dependent strains in the high performance concrete were lower than that of the normal strength concrete and showed less variation, suggesting a more uniform microstructure in high performance concrete. (Lopez *et al.* 2007). The main cause of strength reduction lies in a weak bonding between cement paste and aggregates. The aggregate sizes have a negative impact on bonding. For any given water/cement ratio, the bonding surfaces decreases with increasing aggregate sizes. A high stress concentration occurs at the interface between cement paste and larger size particles lowering the overall concrete compressive strengths (Chen and Liu 2007). Meanwhile, researchers suggest that the compressive strength of high performance concrete can be related to the maximum packing of aggregate particles (Huang 2006). In the actual concrete construction practice, aggregates usually

* Corresponding author, Ph.D., E-mail: ewang@must.edu.tw

deposit at the bottom resulting in a low homogeneity because of poor mix design, inadequate compaction, or excessive water added to fresh concrete in an attempt to improve workability on site (Wang and Wang 2004). Owing to differences in specific gravity, the aggregate tends to sink towards the bottom of the formwork, creating an insufficient area between aggregates for bonding cement paste. Because the bleeding of the cement paste flushes through spaces between particles, the required aggregate particle packing cannot be fully developed, which leads to a lower than expected concrete strength.

To rectify the problem, engineers and researchers place their focus on developing measuring tools. The recent advancement of the digital image process and analytical software that provides high-speed processing and accurate assessment (Ozturk and Baradan 2008) enable researchers to quantitatively analyze the distribution of aggregates (Mertens and Elsen 2006) and air void (Jana 2007). A direct method, the chromatographic method combining digital cameras and photo image processing of section cuts from concrete experiments, has been developed to study the porosity of concrete with great success (Huang *et al.* 2010a, 2010b). A digital image is created with respect to its spatial coordinate and brightness. In other words, digital images can also be expressed in a matrix format with values in rows and columns. The digital matrix is also referred to as an image element, a picture element, or a pixel. The basic structure of the image processing system consists of five parts: input, output, storage, external communication and mainframe units (Gonzalez and Woods 2008). This paper proposes an image method and reports the study of quantifying the specific surface area of aggregates randomly taken from drilled cores in both horizontal and vertical directions of a 1.0 m³ sample.

2. Experiment and analysis

A pilot test was conducted beforehand to ensure a successful procedure and feasibility in data processing. The procedure for determining the specific surface areas of aggregate particles by the pilot test includes the following steps: (1) separating the aggregate into different standard sieve sizes, (2) placing the aggregate particles in a container and injecting a resin to bind them, (3) sawing the aggregate/resin specimen to obtain one to four cut planes, (4) using an image analyzer to take the aggregate particle images from the cut planes and (5) determining the specific surface areas and other aggregate particle properties, such as the slenderness ratio and the roughness from the images (Wang and Lai 2009). The slenderness ratio of a particle is defined as the ratio of the maximum Feret diameter to the minimum Feret diameter of the particle cross section (Russ 2002). Compared to other more advanced methods (Wang and Frost 2003), the proposed method is applicable in the presence of fine and coarse aggregate when implemented. The pilot test results showed success when utilizing image elements to investigate aggregate distribution, i.e., the variance of concrete in regard to the homogeneity requirement in the code.

2.1 Experimental material and mix ratio

The coarse aggregate, fine aggregate, cement, fly ash, slag, superplasticizers and water used in the test program were obtained from local suppliers. The material properties fully complied with the standard specifications (test standards include CNS61, CNS3036, CNS12549, ASTM C494 TYPE-D, CNS13961, CNS1240). The unit weight components used to cast the high performance concrete

Table 1 Mixture properties of concrete (kg/m^3)

W/b	Water	Cement	Coarse aggregate		Fine aggregate	Fly ash	Slag	SP
			3/8"	3/4"				
0.35	154	225	746	132	897	134	75	7.8

$$f'_c = 280 \text{ kg/cm}^2$$

SP = superplasticizer

Table 2 Properties of fresh concrete

Property items	Values
Unit weight (kg/m^3)	2370
Air content (%)	2
45-minute temperatures ($^{\circ}\text{C}$)	26
Flow time (sec)	35
Slump (cm)	25
Flow slump (cm)	60

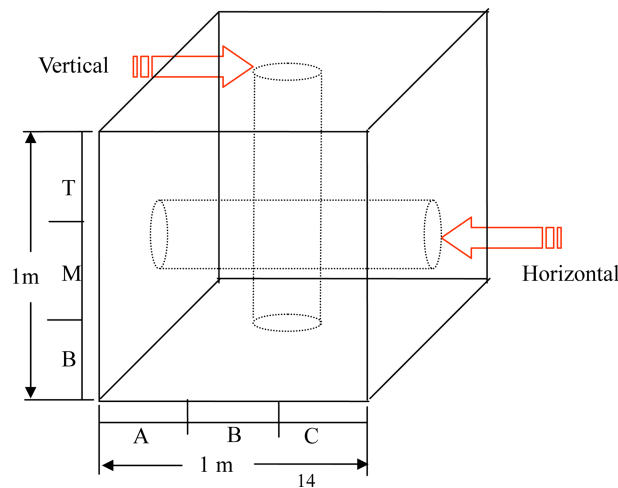


Fig. 1 Drill core schematic in the cubic sample

specimen are shown in Table 1. The fresh concrete was poured into a $1.0 \text{ m} \times 1.0 \text{ m} \times 1.0 \text{ m}$ steel mould. The specimen was cured for seven days and its physical properties are listed in Table 2. After the specimen was ready to test, two cylinders ($15 \text{ cm} \phi \times 100 \text{ cm}$) were drilled; one was taken in the horizontal direction and another one was taken in the vertical direction, as shown in Fig. 1.

2.2 Analysis procedures

The basic steps and test procedures generally followed the well-received digital image processing guidelines. The flowchart of the image process is shown in Fig. 2 (Gonzalez and Woods 2008). A flow chart showing the steps of image element analysis used in this research is shown in Fig. 3.

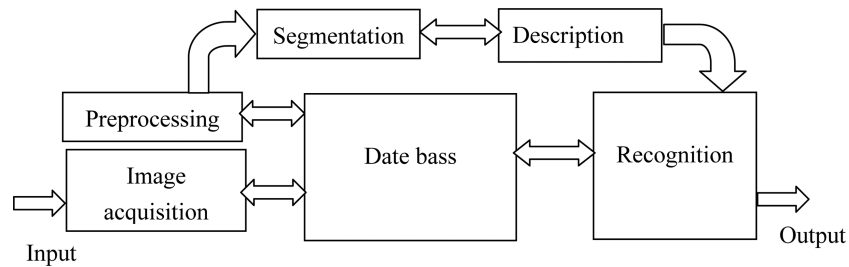


Fig. 2 Basic steps of digital image processing

2.2.1 Image acquisition

Digital cameras having automatic focal length adjustment were used to acquire the aggregate distribution picture and then photocopy to transparent papers. With sufficient light sources, there is no need on histogram adjustment of photos. The coarse aggregate was darkened to differentiate the coarse aggregates from the mortar for further computer recognition. In this research, a digital camera instead of a stereo microscope was used at image acquisition to save time.

2.2.2 Preprocessing

Before the photo image was transformed into digitized information, the resolution of the image was adjusted to 100×116 dpi in order to improve the quality of the image at later processing stages.

2.2.3 Segmentation

Automatic segmentation is one of the difficult tasks in digital image processing. Knowing all objects possess various grey levels, assigning a proper threshold value to distinguish the targeted area or objects from the input image becomes the key feature in the technique. The threshold value is used to identify the aggregate distribution among various gray levels. Fig. 4 shows a typical histogram. It plots the number of pixels in the image (vertical axis) with a particular brightness value (horizontal axis). Algorithms in the digital editor allow the user to visually adjust the brightness value of each pixel and to dynamically display the results as adjustments are made.

2.2.4 Description or feature selection

Commercially available software, Visual Basic (VB) and EasySIGN were used to perform image extraction in the post-processing stage. Various grey levels of image were categorized into two expressions. Those image elements possessing grey levels from 1 to 9 were classified as a single digit symbol "2", while those image elements having grey levels from 10 to 16 were classified as a symbol "-" for ease of extraction.

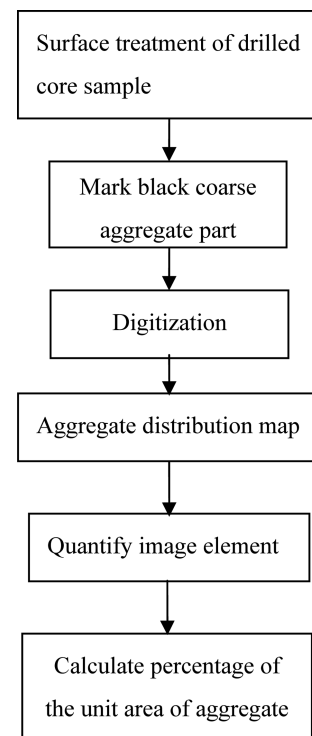


Fig. 3 A flow chart showing the steps of image element analysis

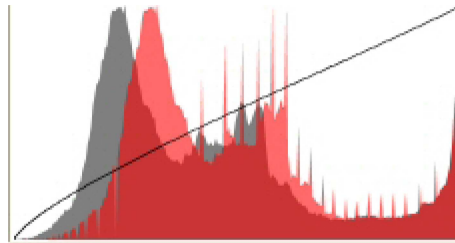


Fig. 4 A typical histogram of photos

Table 3 Aggregate ratio in concrete samples

Direction		Aggregate share (%)			ANOVA
	Position	Top	Middle	Below	
Vertical	<i>P</i>	17.0	16.9	18.0	0.497
	<i>T</i>	5.61	5.16	5.84	0.282
Direction		A	B	C	ANOVA
	Position				
Horizontal	<i>P</i>	19.2	25.9	26.6	3.336
	<i>T</i>	6.46	8.70	8.95	1.120

*ANOVA of vertical and horizontal samples 4.071.

**P*: share of local aggregate image element, %.

**T*: share of total area image element, %.

Table 4 Drilled core samples of compressive strength (MPa)

Direction	Age (Days)				
	28	90	120	180	210
Vertical	39.2	41.7	43.9	48.0	49.5
Horizontal	49.0	51.0	53.2	56.8	60.6

2.2.5 Recognition

This is the process of designating a marker for an object according to information provided. Here, “2” is a darker part, denoting aggregate within a sample; while “-” is the blank portion, denoting the cement mortar part within the sample.

2.2.6 Output and storage

The final image output apparatus includes printers, plotters, or computer screens. The final image obtained from the camera can be subdivided into $m \times n$ picture element pixels having a grey level assigned. The analog image can be further transformed into grids, such as $640 \times 480 \times 255$. It represents a 640×480 picture element pixel with grey levels ranging from 1 to 255. The darkest level is 0 and the brightest is 255. The data can be stored on a disc or on a hard drive in a computer.

2.3 Quantitative calculation method

The quantified aggregate distribution map can be divided into two parts:

- (1) Area: denotes the total amount of image elements obtained from the matrix area.
- (2) Aggregate area: denoted by preset - "2", one digit expresses one image element. The total aggregate ratio per unit area is obtained using Eq. (1) as follows

$$\text{Aggregate ratio per unit area} = \frac{\text{Aggregate amount in image elements}}{\text{Total amount of image elements}} \times 100\% \quad (1)$$

3. Analysis of results

The cut surface was taken by random sampling. The cross-sectional area of particles was also found scattered. The results of aggregate homogeneity were analyzed as follows:

3.1 Aggregate homogeneity analysis

3.1.1 Delineation

Two drilled core samples of cubic specimens were taken in both vertical and horizontal directions after curing. The observed surface was cut at length to a diameter ratio roughly equaling 0.5. The coarse aggregate and foam distribution of the drill cores cut in vertical and horizontal directions were captured by delineating as shown in Figs. 5 and 6, respectively. The coarse aggregate at the surface of drilled core specimens demonstrates uniform distribution characteristics. The gradation,

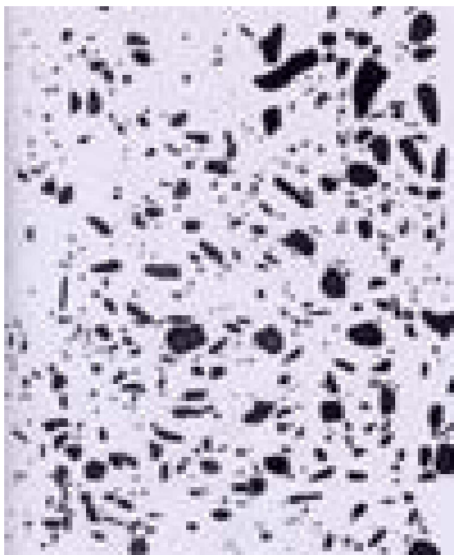


Fig. 5 The aggregate distribution map of vertically drilled core samples

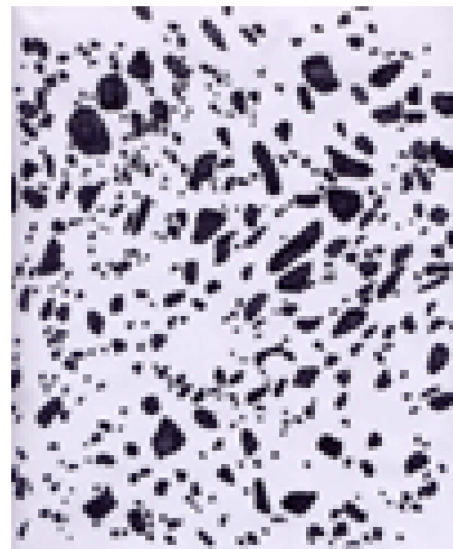


Fig. 6 The aggregate distribution map of horizontally drilled core samples

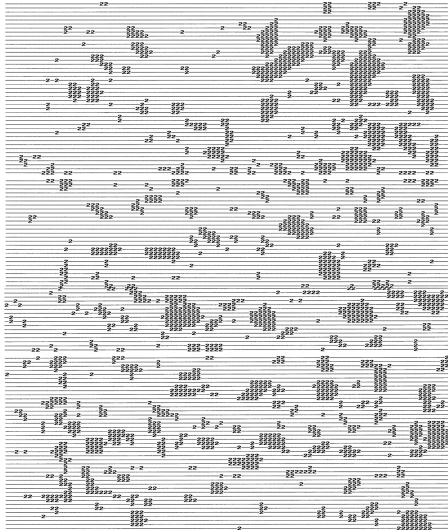


Fig. 7 Aggregate distribution quantification map of vertically drilled core samples in image element analysis

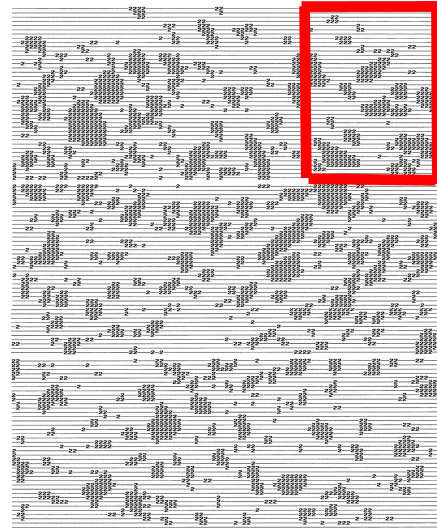


Fig. 8 Aggregate distribution quantification map of horizontally drilled core samples in image element analysis

cleanness and shapes generally comply with current code standard. The porosity was limited between 0.1-0.3 mm, indicating that the high performance concrete quality was satisfactory in homogeneity and densification.

3.1.2 Quantification

The coarse aggregate distribution can be depicted accurately using digital image elements while the share of the coarse aggregate per unit area can also be quantified in the same manner. These are among a few key indicators of a homogenous concrete. The element quantification includes three steps: (1) Highlight the footprint of the coarse aggregate segmentation using pigment on papers before image analyses; (2) Use digital cameras having automatic focal length adjustment function to select the preferred representation in Section A, B and C for optimum performance and (3) Load the

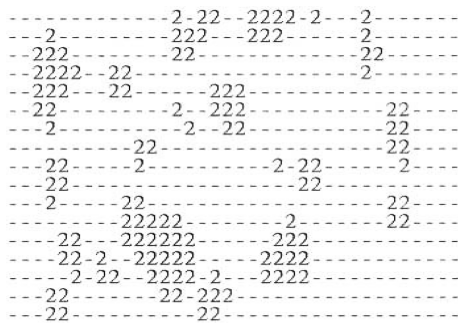


Fig. 9 A close-up view of the area in Fig. 7

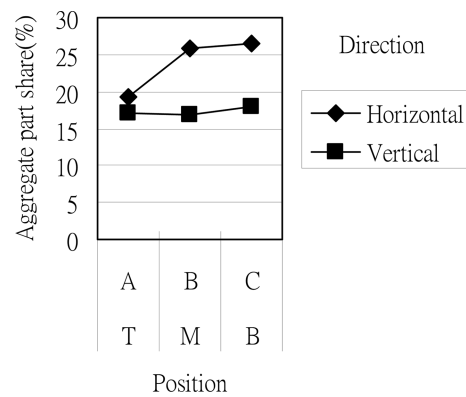


Fig. 10 Aggregate part share in the HPC drill core sample

image file in the computer to calculate amount of the quantified aggregate ratio per unit area using Visual Basic (VB) and a commercial software EasySIGN. The images of the coarse aggregate in the vertical and horizontal directions cut of the experiment, expressed in digitized format were shown in Fig. 7 and Fig. 8, respectively. A closer look at the box view in Fig. 8 is shown in Fig. 9.

3.1.3 ANOVA

ANOVA (analysis of variance) is a collection of statistical models, and their associated procedures to assess the contribution of each variable to the variation. An F -test is constructed by taking the ratio of the “between-groups” variation to the “within-groups” variation. If the between-groups variance is much larger than the within-groups, the F ratio becomes large and the associated p -value becomes small. In this research, the shares of coarse aggregates at the top, middle and bottom layers in vertical samples are 17%, 16% and 18%, respectively, whereas the shares of coarse aggregates at the left, center and right cross sections of horizontal samples are 19%, 25% and 26%, respectively. It is apparent that the ANOVA of shares of coarse aggregate in the vertical direction (0.497) is smaller than the ANOVA of shares of coarse aggregate in the horizontal direction (3.336). A similar phenomenon was observed in the uniformity of aggregate in two directions. This proves that the high performance concrete specimen demonstrates a higher homogeneity of aggregate in the vertical plane than that of the horizontal plane.

3.2 Compressive strengths

It is expected that the compressive strength increases with increasing shares of coarse aggregate in the high performance concrete. Results obtained from the compressive strength tests agreed with the above statement. While the percentile of coarse aggregate in the horizontal core sample is found to be larger than that of the vertical core samples, the corresponding compressive strengths in the horizontal samples are also higher than that of the vertical core samples. Under the same mixture properties of concrete, the drilled core in the horizontal direction exhibiting better particle packing has relatively higher compressive strengths than that of the vertically drilled core sample. Referring to Table 4, the densely packed aggregate increases the integrity of the concrete also in all of its stages.

4. Conclusions

The homogeneity and the share of coarse aggregate in the high performance concrete can be depicted quantitatively using drilled core samples and can be analyzed by digital image elements. The aggregate distribution and area ratios can be quantified such that the percentage of aggregate per unit area and the share can be calculated. These results are key indicators portraying the quality assessment of high performance concrete. The aggregate distribution, expressed in terms of ANOVA, is used to describe the discrepancies in shares of particles. It was found in the tests that the ANOVA in the vertical sample (0.497) is less than that of the horizontal sample (3.336). This implies that a higher homogeneity of aggregate in the vertical plane than that of the horizontal planes usually occurs in the high performance concrete. As a result, the concrete specimen with better particle packing has a relatively higher compressive strength.

Acknowledgments

The authors are grateful for the support of this research by the National Science Council, Republic of China, under contract No. NSC97-2221-E-151-039.

References

- Chen, B. and Liu, J. (2007), "Investigation of effects of aggregate size on the fracture behavior of high performance concrete by acoustic emission", *Constr. Build. Mater.*, **21**(8), 1696-1701.
- Gonzalez, R.C. and Woods, R.E. (2008), *Digital image processing*, 3rd Edition, Prentice Hall, Englewood Cliff, NJ.
- Hwang, C.L., Peng, S.S., Wang, E.H., Lin, S.H. and Huang, S.L. (2010), "A quantitative measurement of concrete air content using image analyses", *Comput. Concrete*, **7**(3), 239-247.
- Hwang, C.L., Peng, S.S., Lin, S.H., Wang, E.H. and Huang, S.L. (2010), "The experimental investigation of general properties for pervious concrete", *Adv. Interact. Multiscale Mech., 1st Conference (AIMM10)*, Jeju, Korea.
- Hwang, C.L. (2006), *Theory and practice of high performance concrete*, Chan's Arch-Publishing Co., Ltd., Taipei. (in Chinese)
- Jana, D. (2007), "A round robin test on measurements of air void parameter in hardened concrete by various automated image analyses and ASTM C457 methods", *Proceedings of the Twenty-Ninth Conference on Cement Microscopy*, Quebec City, PQ, Canada.
- Lopez, M., Kahn, L.F. and Kurtis, K.E. (2007), "Characterization of elastic and time-dependent deformations in normal strength and high performance concrete by image analysis", *Cement Concrete Res.*, **37**(8), 1265-1277.
- Mertens, G. and Elsen, J. (2006), "Use of computer assisted image analysis for the determination of the grain-size distribution of sands used in mortars", *Cement Concrete Res.*, **36**(8), 1453-1459.
- Ozturk, A.U. and Baradan, B. (2008), "A comparison study of porosity and compressive strength mathematical models with image analysis", *Comput. Mater. Sci.*, **43**(4), 974-979.
- Russ, J.C. (2002), *The image processing handbook*, 5th Edition, Publisher CRC Press, Taylor & Francis LLC.
- Wang, H.Y. (1999), "Anti-corrosion property of HPC material interface", *Proceeding of High Performance Reinforced Concrete Anti-Corrosion Strategy Conference*, Kaohsiung, Taiwan, April.
- Wang, H.Y. and Wang, Y.N. (2004), "Study of properties of aggregate particle packing reinforced high performance concrete", *7th Structure Engineering Symposium of Republic of China*, Taoyuan, Taiwan, August. (in Chinese)
- Wang, L.B. and Lai, J.S. (2009), "Quantification of specific surface area of aggregates using an imaging technique", *Int. J. Pavement Res. Technol.*, **1**(2), 13-19.
- Wang, L.B. and Frost, J.D. (2003), "Quantification of aggregate specific surface area using X-ray tomography imaging", *ASCE Geotechnical Special Publication (GSP)*, **123**, 3-17.
- Wang, H.Y. (2008), "Effect of elevated temperatures on properties and color intensities of fly ash mortar", *Comput. Concrete*, **5**(2), 89-100.